


Global Gene Expression Analysis Reveals Complex Cuticle Organization of the *Tribolium* Compound Eye

Qing Chen^{1,†}, Arun Kirshna Sasikala-Appukuttan^{1,†}, Zahabiya Husain¹, Anura Shrivastava^{1,1}, Marla Spain², Edward D. Sandler², Bryce Daines³, Stefan Fischer^{4,2}, Rui Chen ⁴, Tiffany A. Cook^{2,5,*}, and Markus Friedrich^{1,5,*}

¹Department of Biological Sciences, Wayne State University, Detroit, Michigan, USA

²Center of Molecular Medicine and Genetics, Wayne State University School of Medicine, Detroit, Michigan, USA

³Department of Molecular and Human Genetics, Human Genome Sequencing Center, Baylor College of Medicine, Houston, Texas, USA

⁴Evolutionary Biology of Invertebrates, Institute of Evolution and Ecology, University of Tübingen, Germany

⁵Department of Ophthalmological, Visual, and Anatomical Sciences, Wayne State University School of Medicine, Detroit, Michigan, USA

[†]These authors contributed equally to the project.

*Corresponding authors: E-mails: tiffany.cook2@wayne.edu; friedrichm@wayne.edu.

¹Present address: Labcorp Drug Development, Madison, Wisconsin, USA

²Present address: Tübingen Structural Microscopy Core Facility, Applied Geosciences, University of Tübingen, Germany

Accepted: 17 December 2022

Abstract

The red flour beetle *Tribolium castaneum* is a resource-rich model for genomic and developmental studies. To extend previous studies on *Tribolium* eye development, we produced transcriptomes for normal-eyed and eye-depleted heads of pupae and adults to identify differentially transcript-enriched (DE) genes in the visual system. Unexpectedly, cuticle-related genes were the largest functional class in the pupal compound eye DE gene population, indicating differential enrichment in three distinct cuticle components: clear lens facet cuticle, highly melanized cuticle of the ocular diaphragm, which surrounds the *Tribolium* compound eye for internal fortification, and newly identified facet margins of the tanned cuticle, possibly enhancing external fortification. Phylogenetic, linkage, and high-throughput gene knockdown data suggest that most cuticle proteins (CPs) expressed in the *Tribolium* compound eye stem from the deployment of ancient CP genes. Consistent with this, *TcasCPR15*, which we identified as the major lens CP gene in *Tribolium*, is a beetle-specific but pleiotropic paralog of the ancient CPR RR-2 CP gene family. The less abundant yet most likely even more lens-specific *TcasCP63* is a member of a sprawling family of noncanonical CP genes, documenting a role of local gene family expansions in the emergence of the *Tribolium* compound eye CP repertoire. Comparisons with *Drosophila* and the mosquito *Anopheles gambiae* reveal a steady turnover of lens-enriched CP genes during insect evolution.

Key words: *Tribolium*, eye, evodevo, lens proteins, cuticle, gene family evolution.

Significance

The molecular organization of the clear lens cuticle covering arthropod compound eyes has thus far only been characterized in flies. Taking a transcriptome sequencing approach, this study elucidates the cuticle organization of a beetle eye, yielding new insights into lens protein evolution and revealing unexpected fundamental differences in the structural organization of the compound eye periphery between beetles and flies.

© The Author(s) 2022. Published by Oxford University Press on behalf of Society for Molecular Biology and Evolution.

This is an Open Access article distributed under the terms of the Creative Commons Attribution-NonCommercial License (<https://creativecommons.org/licenses/by-nc/4.0/>), which permits non-commercial re-use, distribution, and reproduction in any medium, provided the original work is properly cited. For commercial re-use, please contact journals.permissions@oup.com

Introduction

Understanding the origin of over 1 million insect species of animal biodiversity continues to be a major quest. One important dimension of this endeavor is to elucidate the genetic underpinnings of the numerous adaptive solutions found in insects. High-throughput sequencing approaches have made it possible to address this aspect in efficient ways, surpassing the power of candidate gene approaches. Here, we adopted a transcriptome sequencing approach to expand our understanding of the genetic organization of compound eye development in the red flour beetle *Tribolium castaneum*.

As a global pest of starch depositories, *Tribolium* has been the subject of genetic studies since the first half of the past century (Boyce 1946). Building on these early efforts, *Tribolium* became one of the first insect species to be studied with genomic tools originally developed in *Drosophila* (Sokoloff 1972). Combined with the ease of culturing and relatively fast speed of development, *Tribolium* serves as a powerful satellite organism in insect developmental biology (Brown et al. 2009; Dönitz et al. 2015). In combination with a high-quality annotated genome (Richards et al. 2008; Herndon et al. 2020) and well-developed genetic manipulation protocols (Schinko et al. 2010; Miller et al. 2012; Gilles et al. 2015), the field gained numerous insights into how the body plan differences between *Drosophila* and *Tribolium* have come about through changes in developmental gene regulation (Beeman et al. 1989; Tomoyasu et al. 2005; Ansari et al. 2018). Comparative studies of visual system development have been motivated by the fact that the organization and formation of the compound eyes differ in fundamental ways between *Tribolium* and *Drosophila* (Friedrich 2006). While the compound eyes of *Drosophila* originate from internalized eye antennal imaginal discs, the *Tribolium* compound eyes form from primordium tissue that is embedded in the lateral epithelium of the larval and pupal head (fig. 1c). These differences aside, the early differentiating retina in both species is filled by a regular array of photoreceptor clusters (fig. 1c) that originate sequentially in the wake of a differentiation front that moves from posterior to anterior of the longitudinal body axis (Friedrich 2006).

Candidate gene studies explored how eye formation compares at the gene regulatory level between *Drosophila* and *Tribolium*. As a result, *Tribolium* now constitutes a key reference point in the comparative analysis of visual system development (Koenig and Gross 2020). Although these candidate studies successfully identified commonalities and differences in the genetic programs that direct compound eye development in *Drosophila* and *Tribolium*, much work lays ahead toward a comprehensive characterization of this process in *Tribolium*. As the next step in this direction, we took an RNA deep-sequencing

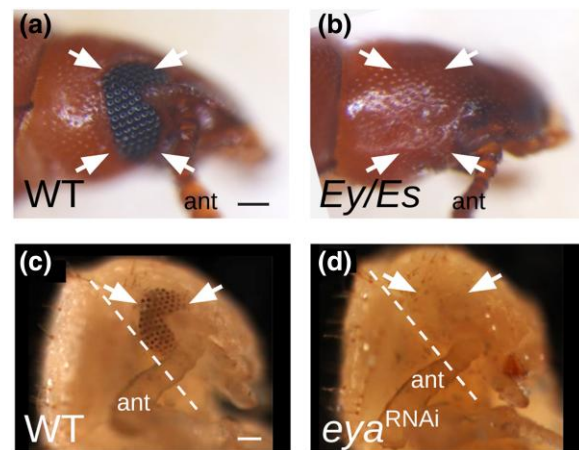


FIG. 1.—External morphologies of WT and eye-depleted adult and pupal heads in *Tribolium*. (a–d) Lateral views with anterior to the right. Ant, antenna. (a) Adult WT adult head. Dorsal and ventral borders of the compound eye are indicated by arrowheads. Scale bar: 100 μ m. (b) Eye-depleted *Ey/Es* mutant adult head. Arrowheads indicate approximate margins of the area filled by the compound eye in WT *Tribolium*. Same scale as in a. (c) Pupal WT *Tribolium* head. Arrowheads indicate the dorsal margins of developing compound eye. Hatched line indicates border between the head and the thorax. Dark brown dots in the differentiating retinal field represent early emerging photoreceptor clusters. Scale bar: 100 μ m. (d) Pupal head of eye-depleted *eya^{RNAi}* animal. Arrowheads indicate the approximate dorsal area filled by the developing compound eye in WT animals. Same scale as in c.

approach and compared the transcriptomes of wild type (WT) and eye-depleted animals at both the pupal and adult stage. The most surprising finding of this effort was the high proportion of cuticle-related genes with enriched expression levels in the developing compound eye of *Tribolium*, the focus of this report.

The complex layered cuticle secreted by epithelial cells is the building material of the arthropod exoskeleton. Previous work elucidated pivotal protein components of this biopolymer, largely defined by the binding of and meshwork formation around chitin (Noh et al. 2016). Previous studies also characterized over ten conserved gene families that encode protein components of cuticle generally referred to as cuticle proteins (CPs; Willis 2010). The two largest CP subfamilies code for CPR RR-1 and CPR RR-2 proteins, which are characterized by the deeply conserved chitin-binding Rebers and Riddiford consensus domain (Rebers and Riddiford 1988; Rebers and Willis 2001). Adding to this complexity of protein domain-defined CP genes, there are several gene families that code for low-complexity proteins, which we will refer to as noncanonical CPs. Although some of the latter are more deeply conserved, the majority are either evolutionarily young or characterized by highly repetitive sequence features that prevent reliable identification of distant

homologs across insect orders (Cornman and Willis 2009). Recent genomic surveys not only confirmed the ancientness of arthropod CP gene families but also detected phylogenetic signal for an expansion of CP diversity at the dawn of insect evolution (Thomas et al. 2020).

At the structural level, CP gene complexity is explained by the existence of specialized cuticle types. The most pervasive distinction is that of tanned body wall cuticle, that is pigmented and hardened (sclerotized; Noh et al. 2016), versus clear and elastic cuticle that forms the flexible connections between segmental units of the arthropod body plan (Willis 2010). In addition, differential CP gene expression and melanin production evolved to furnish adaptive body colorations in insects, ranging from camouflage to aposematic warning colors (Noh et al. 2016; Popadić and Tsitlakidou 2021). Adding further to this diversity, beetles are characterized by heavily sclerotized forewings, the elytra, which cover a pair of ancestrally transparent and flexible hindwings (Dittmer et al. 2012). Moreover, beetles share with other arthropods yet another highly specialized and important cuticle type: the clear cuticle of the corneal lens that covers every single unit of the compound eye, that is the ommatidia (Charlton-Perkins et al. 2011). Major proteomic and gene expression analyses have been conducted to characterize cuticle genes that contribute to the corneal lens cuticle in *Drosophila melanogaster* (Stahl, Charlton-Perkins, et al. 2017), the mosquito *Anopheles gambiae* (Champion et al. 2016; Vannini and Willis 2016; Zhou et al. 2016), and the specialized larval eye of the diving beetle *Thermonectus marmoratus* (Stahl, Baucom, et al. 2017). Combined, these studies converge on documenting the largely cuticular nature of the ommatidial lenses in insects (Stahl, Charlton-Perkins, et al. 2017).

Our transcriptomic, phylogenetic, gene linkage, and functional analyses identify two major CP gene contributors to the *Tribolium* corneal lens cuticle. The most highly expressed CP gene is *TcasCPR15*, which codes for a beetle-specific but pleiotropic member of the ancient CPR RR-2 gene family. The second major CP gene, *TcasCP63*, is less transcript abundant and part of a newly described beetle-specific family of CP genes, documenting the complementary role that gene family expansions play in the emergence of the *Tribolium* compound eye CP repertoire. The remainder of the unexpectedly large number of compound eye DE CP genes is most likely due to enrichment in the pronounced frame of melanized cuticle that surrounds the *Tribolium* compound eye for internal fortification. Our structural studies further identify a third cuticle element in the *Tribolium* compound eye in the form of fine, tanned cuticle frames that outline each lens facet, likely supporting the exterior stability of the exterior *Tribolium* compound eye. Via comparison with the lens cuticle repertoires of *Drosophila* and *Anopheles*, our first analysis of compound eye CP gene use in the compound eye of a beetle species

provides critically expanded insights into the evolutionary turnover of lens CP usage in insects and expands our structural understanding of the *Tribolium* compound eye.

Results

Rich Cuticle Gene Deployment in the *Tribolium* Compound Eye

To identify genes with enriched or specific expression in the mature *Tribolium* compound eye, we deep sequenced RNAseq libraries prepared from adult heads of GAI WT beetles and the mutant strain *Eyeless/Extra Sclerites* (*Ey/Es*), in which the compound eyes are replaced by regular tanned body wall cuticle (fig. 1a and b). Differential transcript enrichment (DE) analysis identified 186 genes with significantly higher transcript levels in the WT adult head compared with eye-depleted *Ey/Es* animals (supplementary 1, P1, Supplementary Material online). This included visual system benchmark genes that have been previously confirmed to be highly compound eye-specific in *Tribolium* such as the photoreceptor-specific ultraviolet (UV) and long wavelength (LW) light-sensitive opsin homologs (Jackowska et al. 2007) and the regulatory transcription factor *Pvull-Pstl* homology 13 (*Pph13*; Mahato et al. 2014; table 1). Further top enriched genes in the adult eye DE gene population included *Arrestin 1* (*Arr1*) and *Arrestin 2* (*Arr2*) (table 1), which execute well-documented Opsin recycling functions in the phototransduction machinery (Wang and Montell 2007).

To identify DE genes for the developing *Tribolium* eye, we prepared transcriptomes from dissected WT pupal head tissues that encompassed the developing compound eye region and the corresponding lateral head tissue in “eye-depleted” pupae (fig. 1c and d). The latter were generated by two RNA interference (RNAi)-mediated knockdown treatments previously shown to abolish compound eye development in *Tribolium* (Yang, Weber, et al. 2009; Yang, Zarinkamar, et al. 2009). One involved the combinatorial knockdown of the functionally redundant retinal determination transcription factor genes *twinn of eyeless* (*toy*), *eyeless* (*ey*), and *dachshund* (*dac*) (*TED*^{RNAi}). The second treatment targeted the retinal determination transcription factor gene *eyes absent* (*eya*^{RNAi}; fig. 1d). Differential transcriptome analyses detected 286 significantly transcript level reduced genes in the *TED*^{RNAi} knockdown transcript population and 174 in the *eya*^{RNAi} knockdown transcript population compared with WT. One hundred and thirty-eight genes overlapped between the two populations and were therefore considered high-confidence pupal compound eye DE genes (supplementary 1, P1, Supplementary Material online).

Like the mature compound eye DE gene population, the high-confidence pupal compound eye DE gene population

Table 1Constitutively Expressed Genes in the *Tribolium* Compound Eye

Functional category	Gene	Locus ID	Gene family	WT adult RPKM	Ey/Es RPKM (Log2diff)	WT pupa RPKM	eya RNAi pupa RPKM (Log2diff)	TED RNAi pupa RPKM (Log2diff)
Photoreceptor	Arrestin 2	Arr2	Arrestins	3,244	35.4 (−6.5)	1,578	24.8 (−6.0)	228.4 (−2.8)
Phototransduction	LW-opsin	LOC661924	GPCR	940	17.4 (−5.8)	150	1.5 (−6.7)	9.4 (−4.0)
Phototransduction	Arrestin 1	LOC657618	Arrestins	264	5.7 (−5.5)	165	2.9 (−5.9)	23.9 (−2.8)
Phototransduction	Chaoptin	chp	Leucine-rich repeat family	146	2.0 (−6.2)	107	3.2 (−5.1)	10.3 (−3.4)
Phototransduction	Transient receptor potential-like	LOC657016	TRP ion channels	113	3.1 (−5.3)	124	1.3 (−6.5)	8.7 (−3.7)
Cuticle	TcasCPR15	LOC659570	CPR_RR-2	599	19.6 (−4.9)	21,902	11.3 (−10.9)	154.6 (−7.2)
Cuticle	TcasCp63	LOC103313848	CP	57	2.8 (−4.4)	10,200	6.62 (−10.6)	223.6 (−5.5)
Cuticle	TcasCPR68	LOC662513	CPR_RR-1	223	19.7 (−3.5)	1,198	359 (−1.7)	190.8 (−2.7)
Cuticle	TcasCPR77	LOC662799	CPR_RR-1	156	29.8 (−2.4)	158	32.6 (−2.3)	31.1 (−2.4)
Undefined	Putative glycine-rich cell wall structural protein 1	LOC107397745	Orphan	142	3.0 (−5.6)	4,786	1.9 (−11.3)	42.5 (−6.8)
Undefined	Glycine-rich orphan gene	LOC103312788	Orphan	822	383.0 (−1.1)	69	10.7 (−2.7)	7.8 (−3.2)

NOTES.—Transcript expression levels in WT pupal and adult heads for genes that were detected as significantly transcript enriched in both, the pupal (WT vs. *eya*^{RNAi}, TED^{RNAi}) and adult (WT vs. *Ey/Es*) transcriptome comparisons, sorted by WT pupal transcript expression levels. Transcript levels are quantified as Reads Per Kilobase of exon per million reads Mapped (RPKM). Transcript-level differences between eye-depleted and WT animals are quantified as binary log fold difference (log2diff) values.

included LW-opsin, UV-opsin, and *Pph13* (supplementary 1, P1, Supplementary Material online and table 1), consistent with their previously reported expression in the developing pupal retina of *Tribolium* (Jackowska et al. 2007; Mahato et al. 2014). Further corroborating the existence of shared DE genes in the mature and developing compound eye transcriptomes, gene pathway and gene function enrichment analyses identified the KEGG pathway term Phototransduction—fly (tca04745) as overrepresented in both the adult and the pupal *eya*^{RNAi} defined DE transcript populations (supplementary 2, table 1, Supplementary Material online). Even more notable, however, was the overrepresentation of the GO term “structural constituent of cuticle” (GO:0042302) in both pupal compound eye DE gene populations, followed by “extracellular region” (GO:0005576), “chitin metabolic process” (GO:0006030), and “chitin-binding” (GO:000806) (supplementary 2, table 1, Supplementary Material online).

Given the preponderance of cuticle-related genes in the pupal compound eye DE gene populations, we explored their relation to the overall CP gene repertoire of *Tribolium*. To this end, we compiled previously annotated *Tribolium* CP genes (Dittmer et al. 2012) and additional genes with cuticle-related nomenclatures from the most recent *T. castaneum* genome assembly (Herndon et al. 2020). This effort resulted in a total of 174 *Tribolium* CP genes (supplementary 1, P2, Supplementary Material online), over 30% (55) of which were identified as high-confidence compound eye DE genes. The latter included members of eight different CP gene families or subfamilies

(supplementary 1, P3, Supplementary Material online) (Willis 2010; Dittmer et al. 2012), indicating a rich and complex use of CP genes in the *Tribolium* compound eye.

Transcriptome Evidence of Constitutively Enriched Compound Eye Cuticle Genes

For the thresholds applied in our enrichment analysis, the transcript levels of 11 genes were significantly reduced in both eye-depleted adults and eye-depleted pupae compared with WT, indicating continuously enriched or specific expression in the *Tribolium* compound eye (table 1). Besides LW-opsin, *Arrestins*, and two *Tribolium*- or Coleoptera-specific genes (LOC107397745, LOC103312788), this included four uncharacterized CP genes: the noncanonical CP gene *Tribolium Cuticle protein 63* (*TcasCp63*) (LOC103313848), the CPR RR-1 homologs *TcasCPR68* (LOC662513) and *TcasCPR77* (LOC662799), and the CPR RR-2 homolog *TcasCPR15* (LOC659570). Among these genes, *TcasCp63* and *TcasCPR15* stood out as the most strongly enriched compound eye CP genes in the WT pupal head while being barely detectable in the eye-depleted conditions (table 1 and supplementary 1, P2, Supplementary Material online).

Expression and Knockdown Validation of *TcasCPR15* and *TcasCp63*

To validate the enriched expression of *TcasCPR15*, *TcasCp63*, *TcasCPR68*, and *TcasCPR77* in the mature *Tribolium* compound eye, we performed semiquantitative

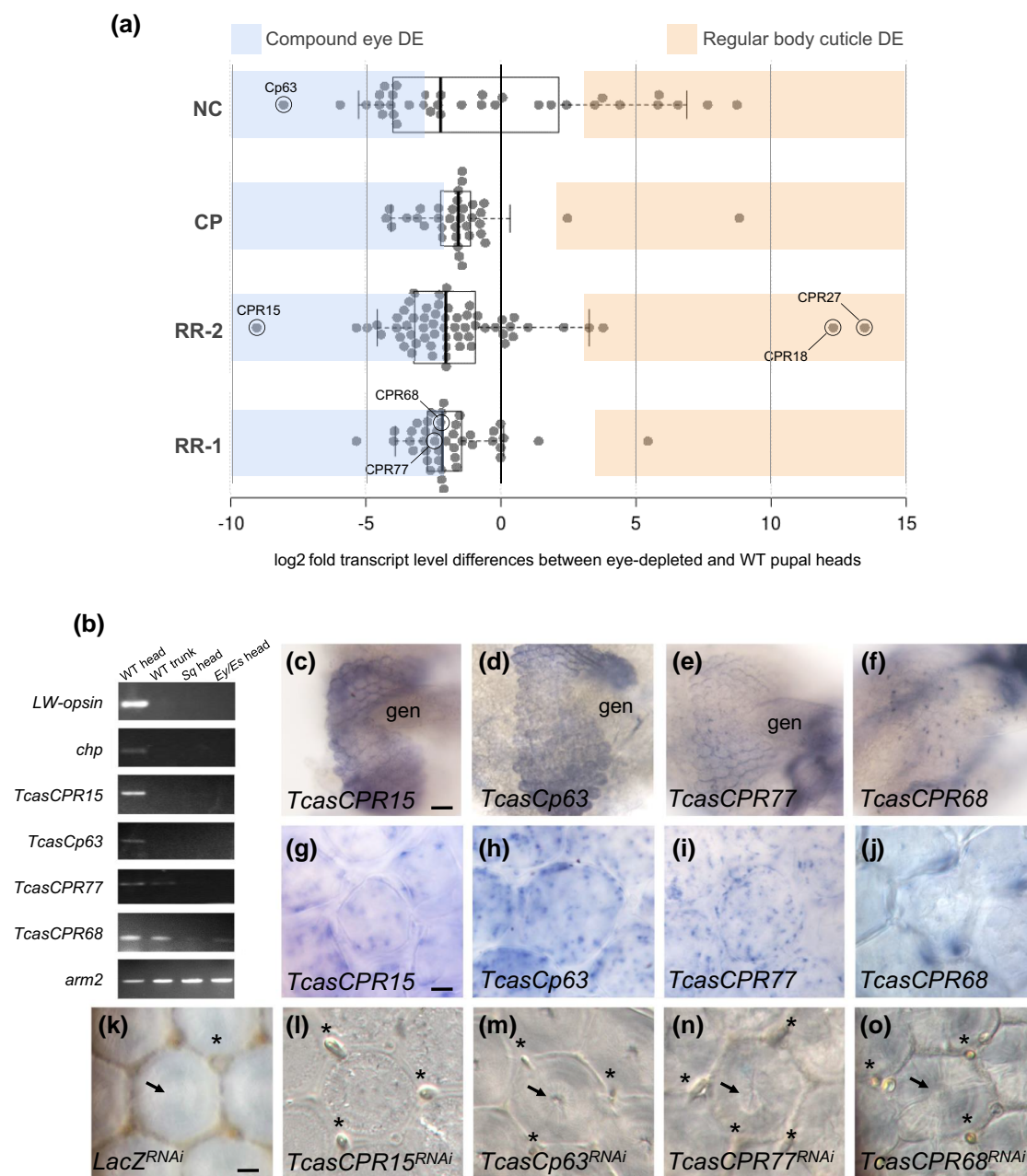


FIG. 2.—Enriched cuticle gene expression in the developing *Tribolium* compound eye. (a) Bee swarm box plot of averaged binary log (log₂) fold differences in cuticle gene transcript levels in *eya*^{RNAi} and *TED*^{RNAi} pupal heads compared with WT pupal heads. Blue overlay indicates range of high-confidence compound eye DE genes based on transcript reduction in eye-depleted pupal heads compared with WT pupal heads. Orange overlay indicates range of cuticle DE genes that are significantly transcript enriched in WT compared with eye-depleted pupal heads. Whiskers extend from 5th to 95th percentile of data point distribution. NC, noncanonical cuticle genes; CP, non-CPR subfamily cuticle protein genes; RR-1, CPR RR-1 subfamily CP genes; RR-2, CPR RR-2 subfamily CP genes. (b) Five microliters of semiquantitative RT-PCR amplicons of *TcasCPR15*, *TcasCp63*, *TcasCPR77*, and *TcasCPR68* from adult stage cDNA preparations from WT head, WT trunk, *sq* head, and *Ey/Es* head tissue separated in 1% agarose gel. RT-PCR amplicons of the photoreceptor-specific benchmark genes *LW-opsin* and *Chp* are shown for comparison. *Armadillo2* (*Arm2*) amplicons visualize relative cDNA input. (c–f) Lateral view of 65% pupal head labeled for *TcasCPR15* (c), *TcasCp63* (d), *TcasCPR77* (e), and *TcasCPR68* (f) expression as detected by colorimetric whole-mount in situ hybridization. The scale bar in c corresponds to 50 μm for d–f. (g–j) High magnification view of distal layer of single ommatidial unit labeled for *TcasCPR15* (g), *TcasCp63* (h), *TcasCPR77* (i), and *TcasCPR68* (j) expression as detected by colorimetric whole-mount in situ hybridization. (k–o) Differential interference contrast microscopy high magnification view of distal layer of single ommatidial units in *LacZ*^{RNAi} (k) versus *TcasCPR15*^{RNAi} (l), *TcasCp63*^{RNAi} (m), *TcasCPR77*^{RNAi} (n), and *TcasCPR68*^{RNAi} (o) knockdown specimens. Asterisks denote ommatidial bristles. Arrows point at the central lens cuticle core, which was not detectable in the *TcasCp63* knockdown specimens (l). The scale bar in panel k corresponds to 10 μm for k–o.

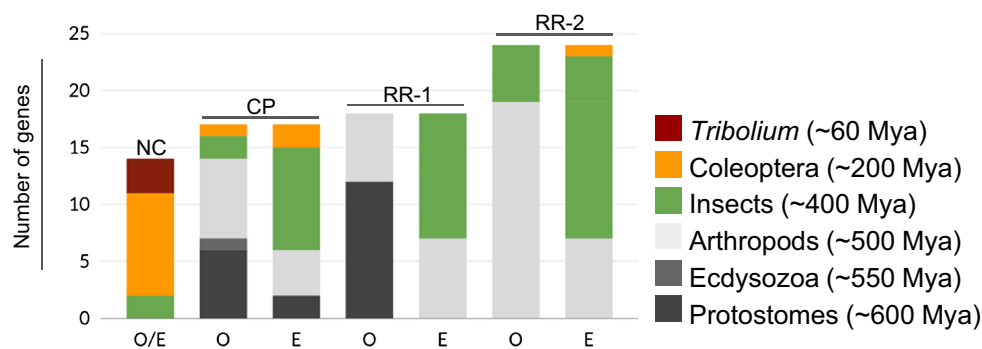


Fig. 3.—Age distributions of compound eye transcript-enriched cuticle genes. Bar graph summarizing time windows of origins for noncanonical, CPR RR-1 (RR-1), CPR RR-2 (RR-2), and other CP genes deployed in the *Tribolium* compound eye. Gene age estimates derived from the OrthoDB (O) (Waterhouse et al. 2013) and Ensembl Metazoa (E) (Kinsella et al. 2011) databases are shown for comparison.

RT-PCR from cDNA isolated from adult WT and eye-depleted *Ey/Es* heads. In addition, we included cDNA from *squint* (*sq*) strain animals, in which the main retina is close to completely missing (Englert and Bell 1963). As positive controls, we analyzed the expression of the photoreceptor-specific benchmark genes LW-opsin and *choptin* (*chp*) (table 1). As expected, *Tribolium* LW-opsin and *chp* were only amplified from WT head cDNA but not from trunk, *Ey/Es* head, or *sq* head cDNA (fig. 2b). The same result was obtained for *TcasCPR15* and *TcasCp63*, thus corroborating the transcriptome evidence of their eye-specific enrichment. *TcasCPR77* was likewise undetectable in *Ey/Es* head or *sq* head cDNA, but its amplification from trunk cDNA indicated expression in other body regions. This was even more clearly the case for *TcasCPR68*, which was amplified at low levels from *Ey/Es* head and *sq* head cDNA (fig. 2b), suggesting expression in nonvisual compartments of the head.

To assess gene expression in the developing compound eye, we carried out whole-mount in situ hybridization experiments. Tissues were sampled starting from 55% pupal development because lens deposition became detectable by differential interference microscopy at 60% of pupal development. The strongest and most eye-restricted transcript signals were observed for *TcasCPR15* and *TcasCp63* in a homogeneous surface layer of the pupal eye (fig. 2c and d). The transcript localization corresponded to the apical regions of the conserved compound eye cell types known to contribute to lens formation in the *Drosophila* eye, that is the four Semper cells, the two primary pigment cells, and the secondary pigment cells (fig. 2g–i) (Cagan and Ready 1989; Friedrich et al. 1996).

TcasCPR77 showed similarly broad expression but at a lower level compared with *TcasCPR15* and *TcasCp63* (fig. 2e). The distribution of *TcasCPR68* expression signal differed from all of these patterns by being present in small, seemingly randomly distributed clusters in the compound eye and in parts of the tracheal system (fig. 2f). High

magnification microscopy located these clusters closely underneath the distal cell layer of the differentiating retina, possibly representing elements of the developing interommatidial bristles that populate the *Tribolium* compound eye (fig. 2j) (Zarinkamar et al. 2011). In further support of this interpretation, reciprocal BLAST identified *TcasCPR68* as a 1:1 ortholog of *Drosophila Cpr49Ah* (supplementary 2, MSA1, Supplementary Material online), which has been implicated in bristle cell development (Mummary-Widmer et al. 2009).

To probe *TcasCPR15*, *TcasCp63*, *TcasCPR68*, and *TcasCPR77* for a role in lens formation, we conducted gene knockdown experiments by injecting sequence-identical dsRNA preparations into late larvae (Miller et al. 2012). All treatments resulted in considerable larval and pupal lethality (supplementary 2, table 2, Supplementary Material online), which was most pronounced for *TcasCPR77* (100%; $n = 10$) and *TcasCp63* (100%; $n = 18$) followed by *TcasCPR15* (82%; $n = 23$) and *TcasCPR68* (50%; $n = 10$). However, in all cases, close to completely developed adults could be dissected from the pupal cuticle, allowing us to study facet morphology and organization. The average size of the lens facets and their hexagonal shapes appeared not significantly altered in the knockdown treatments compared with WT (supplementary 2, table 3, Supplementary Material online). Most conspicuous was the lack of detectable radial lens layer organization in *TcasCPR15^{RNAi}* specimens which could be visualized by high magnification microscopy of WT lens cuticle preparations and appeared only mildly affected in the other knockdown treatments, if at all (fig. 2k–o).

Taken together, our gene expression analyses and knockdown experiments confirmed *TcasCPR15* and *TcasCp63* as major contributors to the lens cuticle in the *Tribolium* compound eye and validated the compound eye enrichment signal in the transcriptome comparisons. The more dramatic effect of knocking down *TcasCPR15* on lens cuticle organization compared with *TcasCp63*,

TcasCPR68, and *TcasCPR77* aligned well with the fact that *TcasCPR15* was characterized as one of the highest WT pupal expression level CP genes (table 1 and supplementary data file 1, P2, Supplementary Material online).

TcasCPR15 Is a Beetle-Specific Paralog of the CPR RR-2 Subfamily

Given the significant roles of *TcasCPR15* and *TcasCP63* in lens cuticle formation, we explored their evolutionary conservation and protein characteristics. *TcasCPR15* had been previously identified as a 145 amino acids long member of the CPR RR-2 gene subfamily (Dittmer et al. 2012). BLAST searches within the *Tribolium* genome revealed that *TcasCPR15* is a singleton paralog on linkage group (LG) 3 of the NCBI *Tribolium* genome assembly (Herndon et al. 2020). Based on reciprocal BLAST results, we identified unambiguous 1:1 orthologs of *TcasCPR15* only within beetles, all of which were characterized by relatively short extensions at both ends of the highly conserved chitin-binding Rebers and Riddiford domain (supplementary data file 2, MSA2, Supplementary Material online). The available evidence thus characterized *TcasCPR15* as a CPR-2 subfamily homolog that most likely originated during coleopteran diversification and did not spawn further paralogs through later gene duplication events.

TcasCp63 Belongs to an Expansive Family of Noncanonical CP Genes

In contrast to *TcasCPR15*, *TcasCp63* coded for a 147 amino acids long noncanonical CP gene. BLAST searches within the *Tribolium* genome revealed the existence of at least 24 paralogs that were concentrated in three clusters (supplementary data file 1, P4, Supplementary Material online). Seventeen members, including *TcasCp63*, were located within a 100-kb long region of LG3. The two smaller clusters were situated on LG8 and LG10. With one exception (XP_008193791: 499 aa), all members of this noncanonical gene family encoded short, nonpolar amino acid-rich proteins ranging from 50 to 150 amino acids in length (supplementary data file 2, MSA3, Supplementary Material online). As the N-terminal amino acid combination, MFK was the most consistently conserved motif across all members, we decided to refer to this newly described gene family as the MFK gene family. Single paralogs were named based on LG association and relative cluster location. In this nomenclature framework, *TcasCp63* was equivalent to *MFK 3–13*.

Surveying the presence of additional compound eye DE genes in the MFK gene family, we noticed that *TcasCp63* was one of five high-confidence compound eye DE MFK paralogs that were tandem clustered within a 26-kb region on LG3 (supplementary data file 1, P4 and data file 2, MSA3, Supplementary Material online). This finding

suggested that *TcasCp63*, unlike *TcasCPR15*, represented the product of a local and most likely relatively recent gene family expansion. In further support of this notion, preliminary BLAST searches detected similarly clustered 1:1 orthologs in the closely related *Tribolium madens* (NW_025401069), while relationships to *MFK* homologs detected in the Emerald ash borer (*Agrilus planipennis*) genome assembly (GCF_000699045.2) could not be established with high confidence.

The Majority of *Tribolium* Compound Eye Enriched Cuticle Genes Are Ancient

Our findings indicated that the large repertoire of CP genes deployed in the *Tribolium* compound eye was the result of different evolutionary origination mechanisms: local gene family expansions as in the case of *TcasCp63* versus the conserved use of ancestrally eye-deployed CP genes or the transcriptional recruitment of ancient CP genes, which was more applicable to *TcasCPR15*. To gauge the relative contributions of these trajectories, we surveyed CP gene ages in the gene family databases OrthoDB (Waterhouse et al. 2013) and Ensembl Metazoa (Kinsella et al. 2011). To increase sensitivity, we included CP genes that were significantly transcript reduced in at least one of the two pupal knockdown treatments, that is tentative compound eye CP genes, in addition to the high-confidence compound eye CP genes. Combined, this totaled 78 genes, most of which (73) were accounted for in OrthoDB (supplementary 1, P5, Supplementary Material online) (Waterhouse et al. 2013).

Although OrthoDB (Waterhouse et al. 2013) and Ensembl Metazoa yielded identical gene ages for all noncanonical CP genes, Ensembl Metazoa indicated younger gene ages for most members of the canonical CP gene families (fig. 3). This difference notwithstanding, the two databases converged on suggesting that 95% of the canonical compound eye DE CP genes predated the last common ancestor of beetles. As the noncanonical genes accounted for little more than 20% of the surveyed compound eye DE cuticle genes, these results suggested that the transcriptomic compound eye enrichment signal of most CP genes was due to transcriptional recruitment of ancient genes or continued use of ancestrally eye-deployed genes.

Phylogenetic Relationships and Genomic Linkage of Compound Eye DE CPR Genes

To scrutinize the gene age survey evidence that ancient CP genes played the major role in the evolution of the rich *Tribolium* compound eye CP gene repertoire, we probed for phylogenetic signals of adaptive gene family expansions in the CPR RR-1 and CPR RR-2 subfamilies. To this end, we generated maximum likelihood trees for the CPR homologs from *T. castaneum*, and representative CPR homolog samples from *D. melanogaster* and *A. gambiae* (Cornman

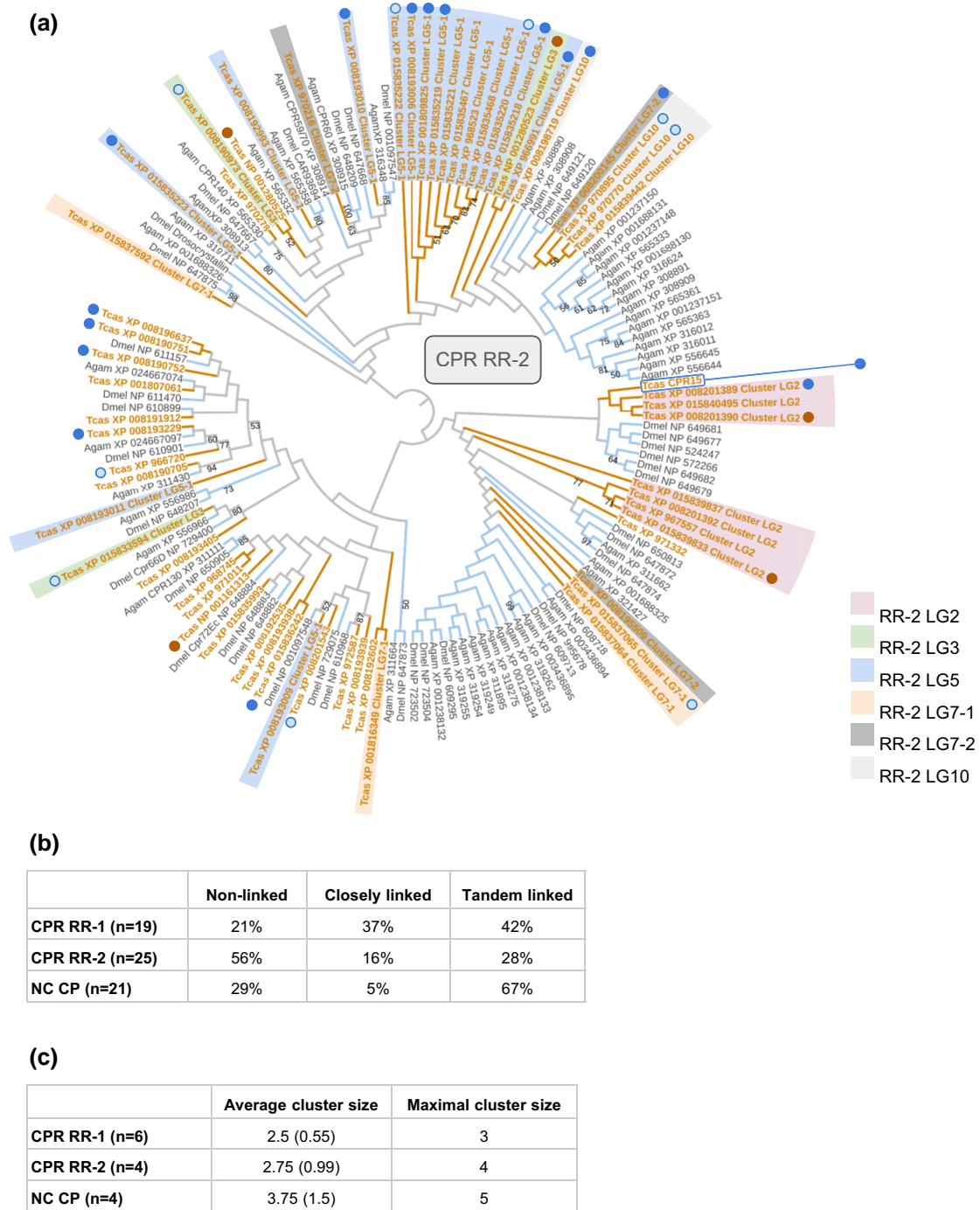


Fig. 4.—Genomic linkage and approximate phylogenetic relationships of compound eye-enriched CPR genes. (a) Maximum likelihood gene tree of the CPR-RR2 gene family members from *T. castaneum* (Tcas), *A. gambiae* (Agam), and *D. melanogaster* (Dmel). Topology unscaled and midpoint rooted. Internal branches with bootstrap support below 60 lack branch support value numbers. Dipteran homologs are indicated by blue branches. Homolog gene cluster associations are visualized by differential background colors specified by the color at bottom right. *Tribolium* homologs are indicated by brown branches and protein identification numbers. High confidence *Tribolium* compound eye DE genes are indicated by terminal blue dots. Tentative *Tribolium* compound eye DE genes are indicated by light blue dots with dark blue margins. The major lens cuticle gene *TcasCPR15* is highlighted by a blue margin and extended blue dot. Body wall cuticle *Tribolium* DE genes are indicated by brown dots. Searchable tree accessible at: <https://itol.embl.de/tree/141217516110951620682560>. See figure 1 in supplementary 2, Supplementary Material online for CPR RR-1 tree and gene cluster visualization. (b) Physical linkage of high-confidence and tentative compound eye DE paralogs (gene numbers given in parentheses) in CPR and noncanonical CP gene families. Closely linked paralogs are defined as separated by interspersed genes from other gene families. (c) Comparison of average and maximal cluster sizes of high-confidence and tentative compound eye DE paralogs in CPR and noncanonical gene families. Numbers in parantheses represent standard deviations.

et al. 2008; Togawa et al. 2008). As in previous studies (Cornman and Willis 2008), only few paralog relationships were resolved with high branch support (fig. 4a and supplementary 2, fig. 1, Supplementary Material online), due to the low number of phylogenetically informative sites in the Rebers and Riddiford domain and the phylogenetic depth represented by the CPR gene family.

Given the limited resolution of the CPR gene trees, we also probed for genomic evidence of CPR subfamily expansions in the form of preserved gene clusters generated by repeated rounds of tandem gene duplications. Surveying CPR gene positions in the 10 LGs of the *Tribolium* genome, we detected 18 nonlinked CPR genes, 6 tandem gene duplicates, and 73 homologs that were part of larger gene clusters (supplementary 1, P6, Supplementary Material online).

The nonlinked CPR genes included the major lens cuticle gene *TcasCPR15* although the CPR RR-2 gene tree provided tentative support for a close relationship of *TcasCPR15* to homologs of a seven paralog CPR RR-2 gene cluster on LG2 (fig. 4a). The largest CPR RR-2 gene cluster (RR-2 LG5) comprised 16 paralogs, 7 of which represented high-confidence compound eye DE genes that were spread out over the cluster together with 2 tentative compound eye DE paralogs (fig. 4a and supplementary 1, P6, Supplementary Material online). A similar spread of compound eye DE genes was observed in the largest CPR RR-1 cuticle gene cluster, which was likewise located on LG5 and consisted of 21 paralogs (supplementary 1, P6 and supplementary 2, fig. 1, Supplementary Material online).

As a metric for gene cluster association of high confidence and tentative compound eye DE paralogs, we tallied the numbers of nonlinked versus tandem or closely linked CPR paralogs (figure 4b). This approach revealed a noticeable bias toward linkage in the CPR RR-1 compound eye DE gene population with about 20% of nonlinked paralogs versus 80% tandem or closely linked paralogs (fig. 4b). The CPR RR-2 compound eye DE gene population, in contrast, was characterized by similar fractions of linked (44%) and nonlinked (56%) paralogs (fig. 4b). The analysis further uncovered that CPR RR-1 and CPR RR-2 compound eye DE gene clusters were generally small, not exceeding four paralogs (fig. 4c). Combined, these findings revealed a detectable contribution of localized gene family expansions in the emergence of compound eye DE CPR genes, but discounted a predominant role for localized gene family expansions in the origin of the compound eye DE CPR genes.

Phylogenetic Relationships and Genomic Linkage of Noncanonical Compound Eye DE Cuticle Genes

Given the gene family expansion association of *TcasCp63* and the generally younger ages of noncanonical CP genes (fig. 3), we also investigated the effect of gene family expansions in the emergence of compound eye DE genes throughout the

noncanonical CP gene population. BLAST searches identified 11 previously undefined noncanonical CP genes in the *Tribolium* genome that were related to CP genes in our initial compilation (supplementary 1, P4, Supplementary Material online). Subsequent analyses of multiple sequence alignments established that the noncanonical CP gene population was composed of seven singleton homologs and seven larger gene families with up to eight members in addition to the 25 paralog large MFK gene family. Surveyed across all noncanonical CP genes, the partition of tandem linked compound eye DE genes was notably larger (67%) than in the CPR gene populations (CPR RR-1: 42%; CPR RR-2: 28%) (fig. 4b). Also, compound eye DE gene cluster sizes averaged to a slightly larger number (3.75) in the noncanonical CP genes compared with the two CPR gene subfamilies, that is 2.5–2.75 (fig. 4c). These findings suggested that the emergence of the noncanonical compound eye DE CP genes was more strongly driven by localized gene family expansions than in the CPR genes.

Pleiotropy of *Tribolium* Compound Eye Cuticle Gene Based on High-Throughput Genes Knockdown Evidence

In a final effort to gain insight into the emergence of the *Tribolium* compound eye cuticle gene repertoire, we considered the possibility that the relative contributions of eye-specific gene family expansions versus gene recruitment might also be distinguishable at the level of genetic pleiotropy. Specifically, adaptive gene family expansions can be envisioned to produce compound eye-specific DE genes with no or few functions outside the compound eye, whereas the recruitment of preexisting cuticle genes should be reflected in higher levels of genetic pleiotropy due to the retention of ancestral functions. Prompted by this rationale, we surveyed our compilation of CP genes for embryonic, pupal, and adult gene knockdown effects documented in the iBeetle-Base compilation of *Tribolium* gene knockdown phenotypes (Dönitz et al. 2015; Schmitt-Engel et al. 2015). For the 155 cuticle genes documented in iBeetle-Base at the time, 71 (45%) were recorded with no detectable phenotype, 18 (12%) with mild phenotypes (<20% lethality), and 66 (43%) with strong phenotypes (>20% lethality). The last category included 35 cases of lack of embryonic cuticle (supplementary 1, P7, Supplementary Material online).

Consistent with the expectation that gene pleiotropy and essentiality increase over evolutionary time, the fractions of cuticle genes with reported gene knockdown phenotypes were conspicuously higher in the populations of ancient CP gene families (>50%) compared with the population of younger noncanonical CP genes (25%) (supplementary 2, fig. 2, Supplementary Material online). Well-aligned with these trends, *TcasCp63* was reported without detectable knockdown phenotype in iBeetle-Base (<https://ibeetle-base.uni-goettingen.de/details/TC003058>),

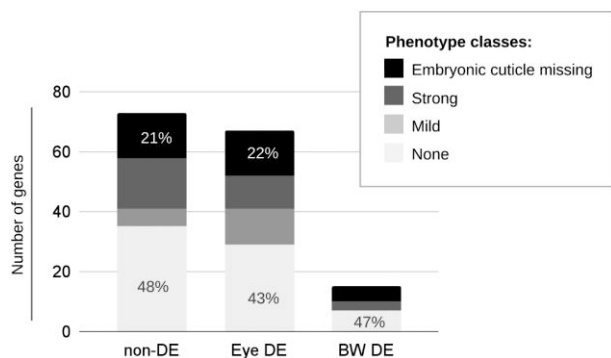


Fig. 5.—Gene criticality related to cuticle gene enrichment classes. Bars show number of genes with no, mild, strong, and embryonic cuticle depletion phenotypes in the iBeetle-Base high-throughput RNAi screen (Schmitt-Engel et al. 2015) parsed by DE classes. Eye DE: high-confidence and tentative compound eye DE genes. BW DE: high-confidence body wall cuticle DE genes.

whereas the knockdown of *TcasCPR15* caused a lack of embryonic cuticle formation (<https://ibeetle-base.uni-goettingen.de/details/TC003109>). Most importantly, compound eye DE CP genes, body wall DE CP genes, and the fraction of nondifferentially expressed CP genes were comprised of similar proportions of genes with reported knockdown phenotypes, ranging above 50% (fig. 5). Also the proportions of genes with embryonic cuticle depletion knockdown phenotypes were very similar in the high-confidence compound eye DE cuticle and the nondifferentially expressed cuticle gene populations, that is 21% and 22%, respectively (fig. 5). These findings were consistent with the scenario that the *Tribolium* compound eye DE cuticle genes originated to a large extent via the deployment of ancient pleiotropic genes as opposed to recent, eye-specific gene family expansions or de novo origination.

Coenrichment of Cuticle Genes in the Compound Eye and Wing Appendages

Given the overall ancient nature of the compound eye DE cuticle genes, we tested their possibly shared deployment in the two types of *Tribolium* wing appendages, that is the heavily sclerotized forewings and the largely transparent hindwings (Tomoyasu et al. 2005, 2009). Previous work in *Tribolium* found that 65% of 131 captured CP genes were expressed at significantly different levels in the fore- and hindwings (Dittmer et al. 2012). Using this resource, we compared the transcript enrichment signatures of 94 CP genes that were cosampled in the wing CP gene expression study and our compilation of CP genes (supplementary 1, P8, Supplementary Material online). In this population, 58 genes were identified as significantly transcript-enriched in at least one of the three tissues. Only 2 CP genes were detected as uniquely enriched for the compound eye (*TcasCPR75* and *TcasCPR55/56*),

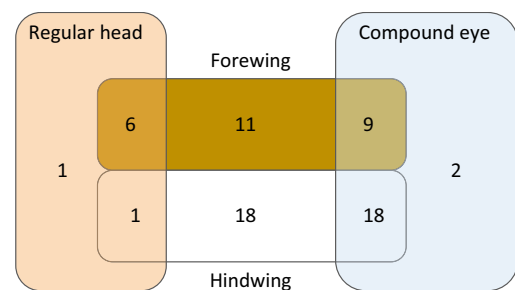


Fig. 6.—Shared versus body compartment-specific cuticle gene enrichment in the *Tribolium* forewing, hindwing, and compound eye. Numbers represent numbers of cuticle genes that are uniquely enriched in the developing compound eye or regular body wall cuticle (regular head) or coenriched in either of the former and the developing fore- or hindwings. See spreadsheet page P8 of supplementary 1, Supplementary Material online for gene identities.

whereas 9 compound eye DE genes were also reported transcript enriched in the forewings versus 18 in the hindwings (fig. 6). The higher overlap of the hindwing and compound eye DE CP genes was consistent with the expectation that these two largely clear cuticle compartments might cutilize CP genes. The existence of CP genes that were coenriched in the compound eye and forewings was more surprising, suggesting the possible existence of shared sclerotized cuticle components in the compound eyes and forewings.

Three Types of Cuticle in the *Tribolium* Compound Eye

The transcriptome evidence for sclerotized cuticle components in the *Tribolium* compound eye prompted us to investigate its cuticle organization in more detail. To this end, we examined preparations of the WT head cuticle after digesting away all cellular tissue. Previous studies of eye pigmentation mutants noted the pronounced black cuticle ridge that surrounds the *Tribolium* WT eye known as the “ocular diaphragm” (OD) (Park 1937; Graham 1957; Sokoloff 1959a; Wolsky and Zamora 1960) (fig. 7a). This structure is completely missing in *Ey/Es*, *eya^{RNAi}*, and *TED^{RNAi}* eye-depleted animals together with the main retina (fig. 1). OD was fully preserved in WT animals after soft tissue removal, confirming its cuticular nature (fig. 7b). Histological sections of the WT eye corroborated the cuticular substance of the OD and revealed its major contribution to the base of the posterior eye (fig. 7c). Moreover, the distinct black coloration of the OD (fig. 7d) indicated fortification through heightened melanin deposition. In support of this notion, we found that the transcripts of melanin production pathway genes were generally enriched in the WT pupal head compared with the eye-depleted conditions (supplementary 2 and table 4, Supplementary Material online). This was most prominently the case for *tyrosine hydroxylase* (*Th*), which represented a high-confidence compound eye DE gene.

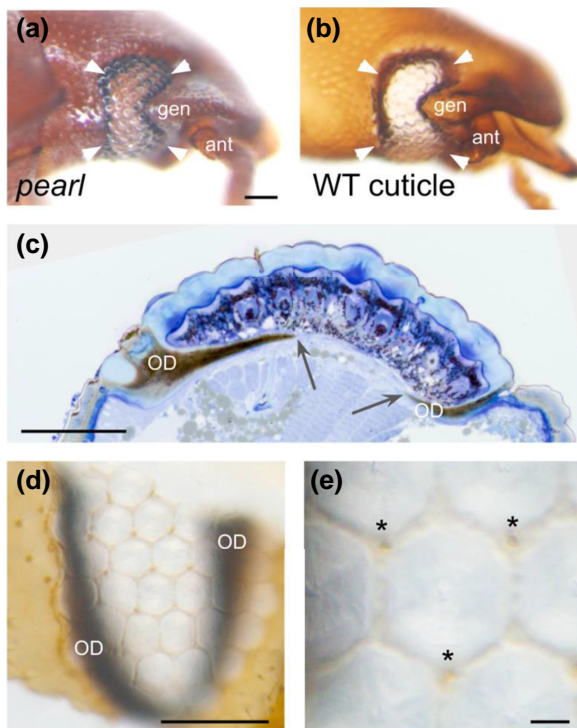


FIG. 7.—Clear, tanned, and melanized cuticle elements in the *Tribolium* compound eye. (a–c) Anterior to the right. (a) The lateral head of live *pearl* mutant *Tribolium* which lacks eye pigment to the effect that the internalized, melanized black cuticle of the OD that furnishes the compound eye margin (arrowheads) is visible. Scale bar: 100 μ m. (b) The lateral head cuticle of soft tissue cleared WT head revealing that the fully preserved OD is part of the cuticular head exoskeleton. (c) Histological section through the WT *Tribolium* compound eye, demonstrating that the OD is a massive internal protrusion at the compound eye margin that reaches underneath the retinal floor. Arrows point at internal edges of the OD. Scale bar: 100 μ m. (d) Horizontal overview of the ventral compound eye cuticle revealing a grit of hexagonal tanned cuticle margins around each facet. Scale bar: 100 μ m. (e) High magnification view of a single facet and its frame of tanned cuticle. Asterisks indicate interommatidial bristles. ant, antenna; gen, gena. Scale bar: 10 μ m.

High magnification inspection of the lens cuticle uncovered the existence of a previously unnoticed third cuticle component of the *Tribolium* compound eye by revealing that each lens facet was outlined with a basal hexagonal rim of tanned cuticle (fig. 7d and e).

Discussion

Darkling beetles have been at the forefront of insect CP studies (Andersen et al. 1973; Willis 2018), which, among other things, revealed that soft and hard cuticle regions are characterized by different types of cuticular proteins (Willis 1986). A considerable number of studies examined the differential deployment of CPs in different parts of the insect exoskeleton (Tetreau et al. 2015; Yang et al. 2017;

Zhao et al. 2017; Liu et al. 2018; Li et al. 2019; Wang et al. 2019), including the compound eye (Vannini and Willis 2016; Stahl, Baucom, et al. 2017; Stahl, Charlton-Perkins, et al. 2017). The overall picture emerging from these studies is that diverged structural cuticle elements are built from different mixtures of evolutionarily ancient cuticle genes. This recognition is clearly corroborated by the large number of ancient and pleiotropic cuticle genes deployed in the *Tribolium* compound eye. In addition, our studies provide new insights into the structural organization of the *Tribolium* compound eye.

Adaptive Significance of Cuticle Fortifications in the *Tribolium* Compound Eye

Our differential transcriptome and structural analyses identified the OD as a major cuticle component of the *Tribolium* compound eye in addition to the facet lenses (figs. 7 and 8). This structure has been noted in other darkling beetle species (Cucujiformia: Tenebrionidae) (Graham 1957; Sokoloff 1959b, 1959c; Wolsky and Zamora 1960; Dyte and Blackman 1961) and representatives of more distantly coleopteran families, including flat bark beetles (Cucujiformia: Silvanidae) and skin beetles (Bostrichiformia: Dermestidae) (Shaw 1966; Buckley and Muggleton 1982). To the best of our knowledge, it is not established whether the melanin-fortified OD is part of the earliest coleopteran body plan organization. Positional and structural similarities, however, leave little doubt that the OD is homologous to the cuticle-based “circumocular ridge” in other insect orders (Weber 1954; Beutel et al. 2013).

The circumocular ridge serves as an endoskeletal element that provides an attachment surface for mouthpart muscles and insulates the elastic retinal tissue from the internal forces and movements associated with the uptake and processing of food (Beutel et al. 2013). In support of this idea, the circumocular ridge is less pronounced in insects that are specialized in the uptake of liquid diets. As a point in case, in *Drosophila*, the circumocular ridge seems to be replaced by the “pigment rim,” a peripheral layer of condensed pigment cells that are recruited from aborted ommatidia during late pupal development (Lim and Tomlinson 2006). Given the likely evolutionarily derived state of the *Drosophila* pigment rim, our findings identify *Tribolium* as an important model for studying the evolution and development of the ancestral arthropod compound eye margin. At the same time, it will be fascinating to explore the likely correlated trajectories of mouthpart evolution, pigment rim organization, and retina movability in the dipteran lineage to *Drosophila* (Fenk et al. 2022).

We did not functionally test the role of *Th* in the melanization of the OD. Previous studies, however, produced evidence that *Th* is involved in the overall hardening of the compound eye cuticle (Gorman and Arakane 2010).

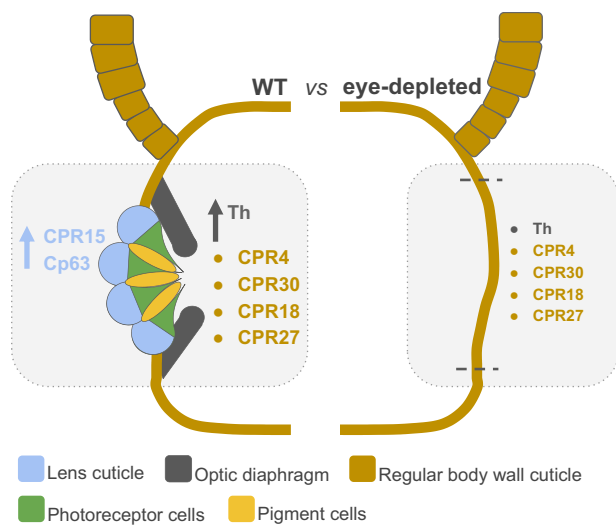


FIG. 8.—Structural model of differential transcript enrichment in eyed versus eye-depleted *Tribolium* heads. Simplified schematic of major cuticle elements in eyed (WT) versus eye-depleted head. Genes hypothesized to be enriched in the compound eye due to differential transcriptional activation (*TcasCPR15*, *TcasCP63*, and *Th*) are indicated by vertical arrows pointing up. CP gene products hypothesized to be enriched in the compound eye due to structural enrichment in the optic diaphragm are indicated by bullet points. Smaller font sizes used for these gene names in the eye-depleted condition reflect the smaller structural representation compared with WT condition. Hatched grey horizontal bars in the lateral cuticle of the eye-depleted head indicate the approximate extent of the missing compound eye area.

Future studies are needed to clarify whether strong melanization is a general state of the insect circumocular ridge. Alternatively, the degree of melanization could correlate with the strength of preferred solid food diets or protect the retinal tissue from external impacts in long-lived, substrate-dwelling species like *Tribolium* (Rivera et al. 2020). The newly discovered tanned cuticle margins of the *Tribolium* facet lenses also speak to the theme of exoskeletal fortification. Like the OD, these elements are missing from cuticle preparations of the *Drosophila* compound eye (data not shown). Pronounced sclerotized facet lens cuticle margins, however, have been described in scarab and fungus beetles (Caveney et al. 1981; Mishra and Meyer-Rochow 2006) and noted in lens cuticle organization in *A. gambiae* (Zhou et al. 2016), inviting broader comparative functional studies.

Structural Versus Gene Regulatory Transcript Enrichment in the *Tribolium* Compound Eye

Two basic scenarios can be envisioned to lead to transcript enrichment of cuticle genes in WT versus eye-depleted *Tribolium* heads. For one, select cuticle genes may be compound eye-specific, most obviously due to employment in the compound eye-specific lens cuticle. This category of organ-specific compound eye DE genes is predicted to be

characterized by the virtual absence of RNAseq traces in the eye-depleted condition, as is the case for the photoreceptor-specific benchmark genes in our data set (table 1). Alternatively, cuticle genes may be detected as eye-enriched due to higher structural representation in the cuticle-fortified compound eye compared with the lateral head cuticle in the eye-depleted samples (figs. 1 and 8). Most obviously, this could be the case for CP genes contributing to the OD, which, based on descriptions of the histology of circumocular ridge (Weber 1954), is likely secreted from infolding sheets of epidermal cells along the margin of the compound eye. In contrast to compound eye-specific DE genes, structurally enriched compound eye-specific DE genes are also expected to be expressed at detectable levels in the heads of eye-depleted animals.

As proof of principle example for the structural enrichment scenario, we noted that the *Tribolium Chitin synthase gene 1* (*Chs1*), which is specifically required for chitin production in the body wall cuticle (Arakane et al. 2005), constitutes a tentative compound eye DE gene. Although reduced in both pupal eye-depleted conditions, and at significant levels in the *eya^{RNAi}* pupae compared with WT, *Chs1* was still detected at high transcript levels (>100 RPKM) in the eye-depleted conditions (supplementary 1, P1, Supplementary Material online). Interestingly, the digestive system-specific paralog *Chs2* was barely detectable in all adult and pupal head transcriptomes (supplementary 1, P1, Supplementary Material online), consistent with the removal of the pharynx and gut in our preparations.

Similarly, the compound eye-associated transcript enrichment of melanin pathway genes like *Th* might constitute the consequence of structural enrichment given the relative size of the melanized OD and the fact that *Th* is deployed throughout the body cuticle at varying concentrations (Gorman and Arakane 2010). On the other hand, the buildup of the visibly higher melanin concentration in the OD very likely reflects higher cellular levels of *Th* activity. This difference thus seems better explained through a third mechanism leading to relative transcript enrichment, that is gene regulatory enrichment, instead of, or in addition to, purely structural enrichment.

Structural enrichment through deployment in the OD, however, remains the most compelling explanation for the detection of well-documented body wall cuticle genes as high-confidence compound eye DE genes in our differential transcriptome analysis (fig. 8). The CPR RR-1 homolog *TcasCPR4*, for instance, which constitutes an abundant component of pore channel fibers in tanned body wall cuticle (Noh et al. 2015), ranked among the most highly expressed genes in the WT pupal head, but was significantly transcript reduced in the eye-depleted pupal heads (supplementary 1, P2, Supplementary Material online). Likewise, the similarly abundant rigid body wall cuticle component *TcasCP30* (Mun et al. 2015) was a top transcript

in the pupal heads but significantly reduced in eye-depleted samples (supplementary 1, P2, Supplementary Material online).

The findings for *TcasCPR4* and *TcasCP30* suggest that the CP composition of the OD and regular head cuticle may be largely equivalent, consistent with their likely shared developmental origins from epithelial cells (Weber 1954). At the same time, it is reasonable to hypothesize the reduction of exocuticle layer components given the apparent fusion of the cuticle sheets secreted by opposing invaginated epithelial cell layers during OD formation (Weber 1954). There are thus developmental and structural reasons for considering the OD a distinct cuticle type that is likely enriched by a different blend of CPs compared with the body wall cuticle.

Interestingly, *TcasCPR27* and *TcasCPR18*, which code for directly interacting RR-2 CPRs that are top abundant in the *Tribolium* forewings (Noh et al. 2014, 2016), were top transcript-enriched in the eye-depleted pupal heads but below detection level in the WT samples (supplementary 1, P2, Supplementary Material online and fig. 2a). However, given that the transcriptional activation of *TcasCPR27* and *TcasCPR18* does not occur before late pupation (Arakane et al. 2012; Sirasoonthorn et al. 2021), which was not captured in our pupal samples, the absence of detectable *TcasCPR27* and *TcasCPR18* RNAseq reads most likely reflects their late transcriptional activation (figs. 2a and 8). The high transcript levels of both genes in the eye-depleted transcriptomes seem best explained by a combined effect of modified temporal regulation and the compensatory expansion of body wall cuticle in the lateral head (figs. 1 and 8).

TcasCPR15, which we identified as the major lens-specific cuticle gene in *Tribolium*, is most likely an example of gene regulatory enrichment. *TcasCPR15* has been reported as mildly forewing-enriched (Dittmer et al. 2012) and is required for embryonic cuticle formation based on iBeetle-Base (supplementary 1, P8, Supplementary Material online), complementing the high postembryonic lethality we observed in *TcasCPR15*^{RNAi} animals (supplementary 2, table 2, Supplementary Material online). Combined, these data characterize *TcasCPR15* as a pleiotropic CP gene that is also deployed in cuticle types outside the corneal lenses. Experimentally, the compound eye enrichment of *TcasCPR15* by differential gene activation is most directly supported by the in situ detection of higher transcript expression levels in the lens-producing cells of the compound eye compared with the surrounding body wall cuticle-producing cells (fig. 2c).

No detectable embryonic phenotypes have been reported for *TcasCp63*^{RNAi} animals in iBeetle-Base (supplementary date file 1, P7, Supplementary Material online), contrasting with the larval and pupal lethality in our postembryonic *TcasCp63* knockdown experiments

(supplementary 2 and table 2, Supplementary Material online). *TcasCp63* may thus constitute a second example of a pleiotropic cuticle gene that is differentially upregulated in lens cuticle-producing cells, despite its likely more recent evolutionary origin.

Ultimate insights into the contribution of lens versus OD expressed genes to the *Tribolium* compound eye DE gene repertoire await proteomic analyses. A complementary approach would be to study the effects of knocking down the *Tribolium* homolog of the transcription factor *Pax2* (LOC656415) on CP gene transcript levels. Although *Pax2* has not yet been studied in *Tribolium* and our transcriptome coverage was too shallow to capture compound eye-related expression differences (supplementary 1, P1, Supplementary Material online), comparative evidence identifies *Pax2* as a promising candidate tool to study differential gene activation in the lens-producing cells of *Tribolium* (Blanco et al. 2005; Charlton-Perkins et al. 2017).

Dynamic Evolutionary Turnover of Insect Lens CPs

Taken together, our gene demographic, phylogenetic, genomic, and gene criticality data lead us to conclude that the great majority of the CP genes utilized in the *Tribolium* compound eye are ancient and also utilized in other areas of the exoskeleton. Only a relatively small number of compound eye DE cuticle genes seem to have originated through recent, potentially adaptive gene family expansions. One of the three cases we detected involves the tandem gene duplication of the CPR RR-1 homologs *TcasCPR22* and *TcasCPR23* (supplementary 1, P6, Supplementary Material online, fig. 1). At the nucleotide level, these sister paralogs differ by 7 replacement and 20 silent substitution differences (data not shown), suggesting continued purifying selection. The much more dramatic sequence diversification of the lens-specific *TcasCp63* and its four tandem-linked compound eye DE MFK gene family paralogs prevented a similar preliminary test for adaptive protein sequence change. In both cases, however, solely an increase in the quantitative contribution to lens cuticle could be adaptive. The latter possibility in turn could be the consequence of an evolutionarily neutral steady-state turnover of CP contributions to the lens cuticle. Fine-grained studies at the population and genus level will be required to discriminate between such scenarios.

These ambiguities notwithstanding, previous studies documented the general complexity of lens cuticle CP mixtures (Vannini and Willis 2016; Zhou et al. 2016; Stahl, Baucom, et al. 2017; Stahl, Charlton-Perkins, et al. 2017). Our finding of at least two lens-enriched CPs in *Tribolium*, that is *TcasCPR15* and *TcasCP63*, together with a large pool of candidate lens-enriched compound DE CP genes, seems consistent with this picture. In *Drosophila*, proteomic studies identified four lens CPs: Drosocrystallin (Dcy), Dmel

Cpr66D, Dmel Cpr47Ee, and Retinin (Stahl, Baucom, et al. 2017). Of these, Dcy constitutes the quantitatively predominant component of the corneal lens, in line with the early discovery of *dcy* as *Drosophila* compound eye lens gene (Komori et al. 1992; Janssens and Gehring 1999; Stahl, Charlton-Perkins, et al. 2017). *Drosophila dcy* represents a Diptera-specific CPR RR-2 homolog thus paralleling the Coleoptera-specificity CPR RR-2 origin of *TcasCPR15*. Given that N:N orthologs of *dcy* do not exist in *A. gambiae* (Vannini and Willis 2016; Zhou et al. 2016), the emergence of *dcy* appears to postdate the early diversification of Diptera. Equally notable, *dcy*, like *TcasCPR15*, is a pleiotropic CP gene, serving as a building block in membrane-support fibers of the digestive system (Kuraishi et al. 2011; Shibata et al. 2015). Although it remains to be explored which of *dcy*'s functions evolved first, these data are compatible with a transcriptional recruitment scenario in which *dcy* acquired its function in the corneal lenses after its emergence and functionalization in the gut epithelium.

The lowest abundant CP in the *Drosophila* lens seems to be Retinin (Stahl, Baucom, et al. 2017). This noncanonical CP, however, is more eye-specific than *dcy* based on MODencode expression data (Chen et al. 2014). This is consistent with the initial biochemical characterization of Retinin as a lens-specific protein (Kim et al. 2008). *Drosophila retinin* has been proposed to be related to the CPLCA gene family of mosquitoes (Cornman and Willis 2009). However, reciprocal BLAST searches using current *D. melanogaster* and *A. gambiae* genome drafts failed to confirm this relationship (data not shown). The combined evidence thus identifies *Drosophila retinin* as a taxonomically restricted noncanonical CP, thus paralleling attributes of the independently originated noncanonical *TcasCp63* of *Tribolium*.

The lens cuticle of *A. gambiae* has been found to incorporate a more balanced mixture of at least 10 CPRs (Vannini and Willis 2016; Zhou et al. 2016). Although this may be partially attributed to the exceptionally dramatic expansions of the CPR RR-1 and CPR RR-2 gene families in mosquitoes and the much more expansive analyses of lens cuticle composition in *A. gambiae* (Champion et al. 2016; Vannini and Willis 2016; Zhou et al. 2016), these data underline the dynamic nature of insect lens cuticle evolution. This is further emphasized by the isolation of low levels of lens proteins in *A. gambiae* that are not CP-related (Zhou et al. 2016), paralleled by the detection of alcohol dehydrogenase in the *Drosophila* lenses (Stahl, Charlton-Perkins, et al. 2017).

Although three sample points from over a million arthropod species discourage sweeping conclusions, it seems reasonable to predict unrelated CP compositions in the lenses of other arthropod subphyla. Overall, the combined insights from *Anopheles*, *Drosophila*, and now *Tribolium*, contrast with the broad taxonomic deployment of two major protein classes (α -, β -, and γ -crystallins) in the lenses of vertebrates (Slingsby et al. 2013). At the same time, vertebrate lens

protein evolution is also characterized by the complementary turnover of other lens protein types via the cooption of housekeeping genes (Wistow 1993; Piatigorsky 1998), which seems to be of lesser significance in insects.

Materials and Methods

Beetle Strains and Husbandry

The *Tribolium* strains GA-I (Haliscak and Beeman 1983), *Ey/Es*, and *sq* were obtained from the Stored Product Insect and Engineering Research unit of the United States Department of Agriculture (Manhattan, Kansas). *Ey/Es* is a translocation of a dominant allele of the *microcephalic* locus from LG5 to LG2 and balanced with the *Es* containing region of LG5 (Sokoloff 1962; Wool 1985; Beeman et al. 1996). The *sq* strain is a spontaneous recessive mutant isolated by Alexander Sokoloff (Englert and Bell 1963). All beetle strains were maintained on a mixture of whole wheat flour, 5% dried yeast, and 0.03% fumagilin at 31 degrees Celsius in constant darkness.

Larval RNA Interference

Larval RNAi was conducted as previously described (Yang, Weber, et al. 2009; Yang, Zarinkamar, et al. 2009). In short, resting-stage larvae were injected with needles drawn from 20- μ l glass microcaps with a Drummond needle puller. Injection solution was prepared by adding dsRNA, water, and 10% phenol red dye with a final concentration of 1 μ g/ μ l of *eya* dsRNA and 2 μ g/ μ l of equimolar amounts of *dac*, *ey*, and *toy* dsRNAs, thus following previously established protocols (Yang, Weber, et al. 2009; Yang, Zarinkamar, et al. 2009). dsRNAs were generated using the MEGAscript T7 kit (Ambion) through bidirectional transcription from PCR amplified template DNAs. Approximately 0.5 μ l of dsRNAs corresponding to *TcasCPR15*, *TcasCP63*, *TcasCPR77*, *TcasCPR68*, and *Escherichia coli LacZ* were injected at 1 μ g/ μ l concentration. Fragments of *TcasCPR15*, *TcasCP63*, *TcasCPR77*, and *TcasCPR68* were amplified by RT-PCR, cloned into pGemT Easy, and verified by Sanger sequencing at the Applied Genomics Technology Center of Wayne State University. See [supplementary table 5 in supplementary 2, Supplementary Material](#) online for primers used in template DNA amplifications.

RNAseq Library Preparation and Sequencing

For pupal samples, 25 heads were dissected in PBS or DMEM + FCS (5%) media. After separation of the head from the thorax, the mouthparts and antennae were removed with fine forceps together with all brain and foregut tissue before transfer into a 1.6-ml Eppendorf collection tube and disruption via micro pestle into Trizol RNA extraction buffer (Invitrogen). For the adult samples, 50 heads were dissociated in the RNA extraction buffer after the removal of antennae.

RNA-seq libraries were prepared as previously described (Daines et al. 2011) and sequenced using the Illumina HiSeq 2,500 platform, generating 33,000,000–43,000,000 reads per sample. The GAI WT-Adult library was single-ended with a read length of 75. All other libraries were paired-end with a read length of 101. Raw sequence reads were deposited to the NCBI Sequence Read Archive with accession numbers SRX819651 (GAI WT pupal head), SRX3118448 (KD^{eya}), SRX3119712 (KD^{TED}), SRX818581 (*Ey/Es* adult head), and SRX818546 (adult GAI head).

Differential Gene Expression Analysis

RNAseq libraries were aligned with HISAT2 (version 2.1.0) to the *T. castaneum* Tcas5.2 genome assembly (GCF_000002335.3) (Kim et al. 2015). Reads were counted per gene, that is sum of all transcripts per gene model, using HTSeq-count (Anders et al. 2015) based on the GCF_000002335.3 GTF feature file and normalized by total library assigned counts to generate RPKM transcript level values. Candidate DE genes and estimates of their degrees and directions of change were identified by fitting positive and negative thresholding curves (fourth-degree polynomial) to encompass 95% of points as rendered by MA plot comparing RPKM values from experimental to untreated control samples, thereby taking into account greater dispersion at lower gene expression levels. For genes with changes outside these boundaries, the degree of change was approximated by the difference between “A” value and threshold value at “M.” The bee swarm box plots of cuticle gene transcript level differences were generated with the online implementation (<http://shiny.chemgrid.org/boxplotr/>) of BoxPlotR (Spitzer et al. 2014).

Go and KEGG Term Analysis

GO analyses of the DE gene populations were performed using the Functional Annotation Clustering Tool from DAVID with default parameters (Huang et al. 2009a, 2009b). All *Tribolium* genes considered in the differential expression analysis were used as the background gene set.

Cuticle Gene Search and Annotation

Cuticle-related genes were identified by searching the RNAseq-supported putative *Tribolium* proteome (Herndon et al. 2020) with the CutprotPfam database motif search tool (Ioannidou et al. 2014), searching genes with the terms “cuticle” or “cuticular” in their NCBI gene annotations, and integrating these genes with the *Tribolium* CP compilation published by Dittmer et al. (2012).

Semiquantitative RT-PCR

Total RNA was extracted from whole pupal and adult heads using the RNAqueous Total RNA Isolation kit (Ambion).

Total RNA sample yields and purities were determined with a NanoDrop 2000c spectrophotometer (Thermo Scientific). Total RNA integrity was evaluated by electrophoresis in a 0.8% agarose gel. For each sample, 1 µg of total RNA was used as input for reverse transcription with the RETROscript kit (Ambion) using random decamer primers. Transcript-specific primers for PCR reactions from cDNA are listed in [supplementary table 5 of supplementary 2, Supplementary Material](#) online. PCR experiments were carried out using GoTaq master (Promega) polymerase following the standard PCR protocol in a Biometra thermocycler with PCR cycle number set to 26. cDNA sample inputs were normalized by comparing amplicon levels of the *Tribolium* housekeeping gene *arm2* (Bao et al. 2012). Amplicons were separated by gel electrophoresis on a 0.8% agarose gel followed by analysis of ethidium bromide-stained bands on a Fotodyne™ imaging workstation.

Whole-Mount In Situ Hybridization

Whole-mount in situ hybridization was performed as previously described with digoxigenin-labeled RNA probes of *Tribolium* *TcasCPR77* (nucleotides 14–776 of NM_001167803), *TcasCPR15* (nucleotides 57–574 of XM_965862), *TcasCP63* (nucleotides 18–437 of XM_008198169), and *TcasCPR68* (nucleotides 18–567 of XM_968604) (Jackowska et al. 2007). DNA templates for in vitro transcription were generated by PCR amplification from plasmid-cloned input DNAs.

Eye Cuticle Preparations and Histology

Selected beetles were terminated by freezing at –20 °C. After thawing, heads were dissected from thorax, cut in half, submerged in PBT, and emptied of residing larger soft tissues with fine forceps. Head cuticles were then incubated in 1 N NaOH at room temperature until total clearance of soft tissues, that is 2 days, before clearing in 100% glycerol.

For histology, beetles were decapitated under room light conditions in a modified Karnovsky fixative solution (Karnovsky 1965), containing 2% formaldehyde and 2.5% glutaraldehyde, buffered with 0.1 M cacodylate (pH 7.4). After the samples were washed in 0.1 M cacodylate buffer (pH 7.4), they were postfixed for 1 h in 1% OsO₄ solution buffered with 0.1 M cacodylate (pH 7.4). The samples were rinsed three times in buffer, followed by three rinses dH₂O followed by dehydration in a graded series of ethanol before being passed through increasing concentrations of Spurr's embedding resin in acetone (3:1, 1:1, 1:3, 100% Spurr). Fresh pure resin (formulated for hard blocks) was used for final embedding and samples were subsequently polymerized at 70 °C for 8 h. For light microscopy, semithin sections at a thickness of 500 nm were cut on a Leica Ultracut UTC

ultramicrotome (Leica Microsystems GmbH, Wetzlar, Germany) with a Histo-Jumbo diamond knife (Diatome, Biel, Switzerland), picked up on glass slides, and stained with an aqueous solution of toluidine blue on a hot plate (60 °C) for 30 s. The sections were imaged using a Zeiss Axioplan microscope, equipped with a Nikon D7100 camera and Helicon Remote 3.6.2.w software (Helicon Soft Ltd, Kharkiv, Ukraine).

Gene Tree Analyses

Multiple sequence alignments for compilations of CPR RR-1 (10.6084/m9.figshare.21778496) and CPR-R2 (10.6084/m9.figshare.21778517) homologs were generated using T-Coffee with default settings (Notredame et al. 2000) (supplementary data file 3, Supplementary Material online). Ambiguous sites were removed with Gblocks using the lowest stringency settings (Castresana 2000). Gene tree estimation was conducted with RAxML within the CIPRES Science Gateway environment (Miller et al. 2011; Stamatakis 2014). Gene trees were rendered and annotated in the iTOL environment (Letunic and Bork 2016).

Supplementary material

Supplementary data are available at *Genome Biology and Evolution* online (<http://www.gbe.oxfordjournals.org/>).

Acknowledgments

The authors thank Sue Brown, Bob Denell, and Sue Haas for providing *Tribolium* stocks, Rob Waterhouse and Livio Ruzzante for help with gene age analysis, Elke Buschbeck for comments on an early version of the manuscript, and the two anonymous reviewers for their generous and impactful comments. This work was supported by the National Science Foundation (IOS grant 0951886 to M.F. and R.C.), the National Eye Institute (grant number R21-EY031526; grant number P30-EY04068 to T.C.) and an unrestricted grant from Research to Prevent Blindness (Wayne State University, Department of Ophthalmology, Visual and Anatomical Sciences) to T.C.

Data Availability

All transcriptome sequence read data are available at the NCBI Sequence Read Archive under accession numbers SRX819651 (GAI WT pupal head), SRX3118448 (KDeya), SRX3119712 (KDTED), SRX818581 (Ey/Es adult head), and SRX818546 (adult GAI head).

Literature Cited

Anders S, Pyl PT, Huber W. 2015. HTSeq—a python framework to work with high-throughput sequencing data. *Bioinformatics* 31:166–169.

- Andersen SO, Chase AM, Willis JH. 1973. The amino-acid composition of cuticles from *Tenebrio molitor* with special reference to the action of juvenile hormone. *Insect Biochem.* 3:171–180.
- Ansari S, et al. 2018. Double abdomen in a short-germ insect: zygotic control of axis formation revealed in the beetle *Tribolium castaneum*. *Proc Natl Acad Sci U S A.* 115:1819–1824.
- Arakane Y, et al. 2005. The PLoS Genet. chitin synthase genes PLoS Genet. and PLoS Genet. are specialized for synthesis of epidermal cuticle and midgut peritrophic matrix. *PLoS Genet.* 14:453–463.
- Arakane Y, et al. 2012. Formation of rigid, non-flight forewings (elytra) of a beetle requires two major cuticular proteins. *PLoS Genet.* 8: e1002682.
- Bao R, Fischer T, Bolognesi R, Brown SJ, Friedrich M. 2012. Parallel duplication and partial subfunctionalization of β -catenin/armadillo during insect evolution. *Mol Biol Evol.* 29:647–662.
- Beeman RW, Stuart JJ, Haas MS, Denell RE. 1989. Genetic analysis of the homeotic gene complex (HOM-C) in the beetle *Tribolium castaneum*. *Dev Biol.* 133:196–209.
- Beeman RW, Stuart JJ, Haas MS, Friesen KS. 1996. Chromosome extraction and revision of linkage group 2 in *Tribolium castaneum*. *J Hered.* 87:224–232.
- Beutel RG, Friedrich F, Yang X-K, Ge S-Q. 2013. Insect morphology and phylogeny: a textbook for students of entomology. Germany: Berlin/Walter de Gruyter.
- Blanco J, Girard F, Kamachi Y, Kondoh H, Gehring WJ. 2005. Functional analysis of the chicken delta1-crystallin enhancer activity in *Drosophila* reveals remarkable evolutionary conservation between chicken and fly. *Development* 132:1895–1905.
- Boyce JM. 1946. The influence of fecundity and egg mortality on the population growth of *Tribolium confusum* duval. *Ecology* 27:290–302.
- Brown SJ, et al. 2009. The red flour beetle, *Tribolium castaneum* (Coleoptera): a model for studies of development and pest biology. *Cold Spring Harb Protoc.* 2009:db.emo126.
- Buckley DS, Muggleton J. 1982. A pearl-eyed mutation in *Oryzaephilus mercator* (Fav.) (Coleoptera, Silvanidae). *J Stored Prod Res.* 18: 31–35.
- Cagan RL, Ready DF. 1989. The emergence of order in the *Drosophila* pupal retina. *Dev Biol.* 136:346–362.
- Castresana J. 2000. Selection of conserved blocks from multiple alignments for their use in phylogenetic analysis. *Mol Biol Evol.* 17: 540–552.
- Caveney S, McIntyre P, Horridge GA. 1981. Design of graded-index lenses in the superposition eyes of scarab beetles. *Philos Trans R Soc Lond B Biol Sci.* 294:589–632.
- Champion MM, Sheppard AD, Rund SSC, Freed SA, O'Tousa JE, Duffield GE. 2016. Qualitative and quantitative proteomics methods for the analysis of the *Anopheles gambiae* mosquito proteome. In: Raman C, Goldsmith MR, Agunbiade TA, editors. Short views on insect genomics and proteomics: insect proteomics, Vol. 2. Cham: Springer International Publishing. p. 37–62.
- Charlton-Perkins M, Brown NL, Cook TA. 2011. The lens in focus: a comparison of lens development in *Drosophila* and vertebrates. *Mol Genet Genomics.* 286:189–213.
- Charlton-Perkins MA, Sandler ED, Buschbeck EK, Cook TA. 2017. Multifunctional glial support by Sempers cells in the *Drosophila* retina. *PLoS Genet.* 13:e1006782.
- Chen Z-X, et al. 2014. Comparative validation of the *D. melanogaster* modENCODE transcriptome annotation. *Genome Res.* 24:1209–1223.
- Cornman RS, et al. 2008. Annotation and analysis of a large cuticular protein family with the R&R consensus in *Anopheles gambiae*. *BMC Genomics* 9:22.
- Cornman RS, Willis JH. 2008. Extensive gene amplification and concerted evolution within the CPR family of cuticular proteins in mosquitoes. *Insect Biochem Mol Biol.* 38:661–676.

- Cornman RS, Willis JH. 2009. Annotation and analysis of low-complexity protein families of *Anopheles gambiae* that are associated with cuticle. *Insect Mol Biol.* 18:607–622.
- Daines B, et al. 2011. The *Drosophila melanogaster* transcriptome by paired-end RNA sequencing. *Genome Res.* 21:315–324.
- Dittmer NT, et al. 2012. Proteomic and transcriptomic analyses of rigid and membranous cuticles and epidermis from the elytra and hindwings of the red flour beetle, *Tribolium castaneum*. *J Proteome Res.* 11:269–278.
- Dönitz J, et al. 2015. iBeetle-Base: a database for RNAi phenotypes in the red flour beetle *Tribolium castaneum*. *Nucleic Acids Res.* 43:D720–D725.
- Dyte CE, Blackman DG. 1961. A pearl-eyed mutation in *Gnathocerus cornutus* (Fab.) (Coleoptera: Tenebrionidae), with notes on similar variants in other beetles. *J Stored Products Res.* 36:168–172.
- Englert DC, Bell AE. 1963. “*Antennapedia*” and “*squint*”, recessive marker genes for linkage group VIII in *Tribolium castaneum*. *Can J Genet Cytol.* 5:467–471.
- Fenk LM, et al. 2022. Muscles that move the retina augment compound eye vision in *Drosophila*. *Nature* 612:116–122.
- Friedrich M. 2006. Continuity versus split and reconstitution: exploring the molecular developmental corollaries of insect eye primordium evolution. *Dev Biol.* 299:310–329.
- Friedrich M, Rambold I, Melzer RR. 1996. The early stages of ommatidial development in the flour beetle *Tribolium castaneum* (Coleoptera; Tenebrionidae). *Dev Genes Evol.* 206:136–146.
- Gilles AF, Schinko JB, Averof M. 2015. Efficient CRISPR-mediated gene targeting and transgene replacement in the beetle *Tribolium castaneum*. *Development* 142:2832–2839.
- Gorman MJ, Arakane Y. 2010. Tyrosine hydroxylase is required for cuticle sclerotization and pigmentation in *Tribolium castaneum*. *Insect Biochem Mol Biol.* 40:267–273.
- Graham WM. 1957. Pearl eye in the confused flour beetle, *Tribolium confusum* duval (Tenebrionidae). *Entomol Mon Mag.* 93:73–75.
- Haliscak JP, Beeman RW. 1983. Status of malathion resistance in five genera of beetles infesting farm-stored corn, wheat, and oats in the United States. *J Econ Entomol.* 76:717–722.
- Herndon N, et al. 2020. Enhanced genome assembly and a new official gene set for *Tribolium castaneum*. *BMC Genomics* 21:47.
- Huang DW, Sherman BT, Lempicki RA. 2009a. Systematic and integrative analysis of large gene lists using DAVID bioinformatics resources. *Nat Protoc.* 4:44–57.
- Huang DW, Sherman BT, Lempicki RA. 2009b. Bioinformatics enrichment tools: paths toward the comprehensive functional analysis of large gene lists. *Nucleic Acids Res.* 37:1–13.
- Ioannidou ZS, Theodoropoulou MC, Papandreou NC, Willis JH, Hamodrakas SJ. 2014. CutProtFam-Pred: detection and classification of putative structural cuticular proteins from sequence alone, based on profile hidden Markov models. *Insect Biochem Mol Biol.* 52:51–59.
- Jackowska M, et al. 2007. Genomic and gene regulatory signatures of cryptozoic adaptation: loss of blue sensitive photoreceptors through expansion of long wavelength-opsin expression in the red flour beetle *Tribolium castaneum*. *Front Zool.* 4:24.
- Janssens H, Gehring WJ. 1999. Isolation and characterization of drosocrystallin, a lens crystallin gene of *Drosophila melanogaster*. *Dev Biol.* 207:204–214.
- Karnovsky MJ. 1965. A formaldehyde glutaraldehyde fixative of high osmolality for use in electron microscopy. *J Cell Biol.* 27:1A–149A.
- Kim E, et al. 2008. Characterization of the *Drosophila melanogaster* retinin gene encoding a cornea-specific protein. *Insect Mol Biol.* 17:537–543.
- Kim D, Langmead B, Salzberg SL. 2015. HISAT: a fast spliced aligner with low memory requirements. *Nat Methods.* 12:357–360.
- Kinsella RJ, et al. 2011. Ensembl BioMarts: a hub for data retrieval across taxonomic space. *Database* 2011:bar030.
- Koenig KM, Gross JM. 2020. Evolution and development of complex eyes: a celebration of diversity. *Development* 147:dev182923.
- Komori N, Usukura J, Matsumoto H. 1992. Drosocrystallin, a major 52 kDa glycoprotein of the *Drosophila melanogaster* corneal lens. Purification, biochemical characterization, and subcellular localization. *J Cell Sci.* 102(Pt 2):191–201.
- Kuraishi T, Binggeli O, Opota O, Buchon N, Lemaitre B. 2011. Genetic evidence for a protective role of the peritrophic matrix against intestinal bacterial infection in *Drosophila melanogaster*. *Proc Natl Acad Sci USA.* 108:15966–15971.
- Letunic I, Bork P. 2016. Interactive tree of life (iTOL) v3: an online tool for the display and annotation of phylogenetic and other trees. *Nucleic Acids Res.* 44:W242–W245.
- Li Z, et al. 2019. Genome-wide identification of chitin-binding proteins and characterization of BmCBP1 in the silkworm, *Bombyx mori*. *Insect Sci.* 26:400–412.
- Lim H-Y, Tomlinson A. 2006. Organization of the peripheral fly eye: the roles of Snail family transcription factors in peripheral retinal apoptosis. *Development* 133:3529–3537.
- Liu B-Q, et al. 2018. Genome-wide identification, characterization and evolution of cuticular protein genes in the malaria vector *Anopheles sinensis* (Diptera: Culicidae). *Insect Sci.* 25:739–750.
- Mahato S, et al. 2014. Common transcriptional mechanisms for visual photoreceptor cell differentiation among Pancrustaceans. *PLoS Genet.* 10:e1004484.
- Miller SC, Miyata K, Brown SJ, Tomoyasu Y. 2012. Dissecting systemic RNA interference in the red flour beetle *Tribolium castaneum*: parameters affecting the efficiency of RNAi. *PLoS One* 7:e47431.
- Miller MA, Pfeiffer W, Schwartz T. 2011. Creating the CIPRES Science Gateway for inference of large phylogenetic trees. In: Proceedings of the 2011 TeraGrid conference: extreme digital discovery. New York: Association for Computing Machinery. Article 41. p. 1–8.
- Mishra M, Meyer-Rochow VB. 2006. Fine structure of the compound eye of the fungus beetle *Neotriplax lewisi* (Coleoptera, Cucujiformia, Erotylidae). *Invertebr Biol.* 125:265–278.
- Mummary-Widmer JL, et al. 2009. Genome-wide analysis of Notch signalling in *Drosophila* by transgenic RNAi. *Nature* 458:987–992.
- Mun S, et al. 2015. Cuticular protein with a low complexity sequence becomes cross-linked during insect cuticle sclerotization and is required for the adult molt. *Sci Rep.* 5:10484.
- Noh MY, Muthukrishnan S, Kramer KJ, Arakane Y. 2015. *Tribolium castaneum* RR-1 cuticular protein TcCPR4 is required for formation of pore canals in rigid cuticle. *PLoS Genet.* 11:e1004963.
- Noh MY, Muthukrishnan S, Kramer KJ, Arakane Y. 2016. Cuticle formation and pigmentation in beetles. *Curr Opin Insect Sci.* 17:1–9.
- Notredame C, Higgins DG, Heringa J. 2000. T-Coffee: a novel method for fast and accurate multiple sequence alignment. *J Mol Biol.* 302:205–217.
- Park T. 1937. The inheritance of the mutation “*Pearl*” in the flour beetle, *Tribolium castaneum* Herbst. *Am Nat.* 71:143–157.
- Piatigorsky J. 1998. Multifunctional lens crystallins and corneal enzymes. More than meets the eye. *Ann N Y Acad Sci.* 842:7–15.
- Popadić A, Tsilakidou D. 2021. Regional patterning and regulation of melanin pigmentation in insects. *Curr Opin Genet Dev.* 69:163–170.
- Rebers JE, Riddiford LM. 1988. Structure and expression of a *Manduca sexta* larval cuticle gene homologous to *Drosophila* cuticle genes. *J Mol Biol.* 203:411–423.
- Rebers JE, Willis JH. 2001. A conserved domain in arthropod cuticular proteins binds chitin. *Insect Biochem Mol Biol.* 31:1083–1093.
- Richards S, et al. 2008. The genome of the model beetle and pest *Tribolium castaneum*. *Nature* 452:949–955.

- Rivera J, et al. 2020. Toughening mechanisms of the elytra of the diabolical ironclad beetle. *Nature* 586:543–548.
- Schinko JB, et al. 2010. Functionality of the GAL4/UAS system in *Tribolium* requires the use of endogenous core promoters. *BMC Dev Biol.* 10:53.
- Schmitt-Engel C, et al. 2015. The iBeetle large-scale RNAi screen reveals gene functions for insect development and physiology. *Nat Commun.* 6:1–10.
- Shaw DD. 1966. The inheritance of two mutations, "pearl" and "fuscous" in *Dermestes maculatus* de Geer (Coleoptera, Dermestidae). *J Stored Prod Res.* 1:261–265.
- Shibata T, et al. 2015. Crosslinking of a peritrophic matrix protein protects gut epithelia from bacterial exotoxins. *PLoS Pathogens.* 11: e1005244.
- Sirasoonthorn P, Kamiya K, Miura K. 2021. Antifungal roles of adult-specific cuticular protein genes of the red flour beetle, *Tribolium castaneum*. *J Invertebr Pathol.* 186:107674.
- Slingsby C, Wistow GJ, Clark AR. 2013. Evolution of crystallins for a role in the vertebrate eye lens. *Protein Sci.* 22:367–380.
- Sokoloff A. 1959a. The "Pearl" gene in *Latheticus oryzae* Waterh. *Am Nat.* 93:394–396.
- Sokoloff A. 1959b. The nature of the "Pearl" mutation in *Tribolium castaneum* herbst. *Am Nat.* 93:329–331.
- Sokoloff A. 1959c. The genetics of "pearl" in *Latheticus oryzae* Waterh. *Can J Genet Cytol.* 1:183–188.
- Sokoloff A. 1962. Linkage studies in *Tribolium castaneum* Herbst. V. The genetics of *Bar eye*, *microcephalic* and *microphthalmic* and their relationships to *black*, *jet*, *pearl* and *sooty*. *Can J Genet Cytol.* 4:409–425.
- Sokoloff A. 1972. The biology of *Tribolium* with special emphasis on genetic aspects. Oxford: Clarendon Press.
- Spitzer M, Wildenhain J, Rappsilber J, Tyers M. 2014. BoxPlotR: a web tool for generation of box plots. *PLoS Genet.* 11:121–122.
- Stahl AL, Baucom RS, Cook TA, Buschbeck EK. 2017. A complex lens for a complex eye. *Integr Comp Biol.* 57:1071–1081.
- Stahl AL, Charlton-Perkins M, Buschbeck EK, Cook TA. 2017. The cuticular nature of corneal lenses in *Drosophila melanogaster*. *Dev Genes Evol.* 227:271–278.
- Stamatakis A. 2014. RAxML version 8: a tool for phylogenetic analysis and post-analysis of large phylogenies. *Bioinformatics* 30:1312–1313.
- Tetreau G, et al. 2015. Analysis of chitin-binding proteins from *Manduca sexta* provides new insights into evolution of peritrophin A-type chitin-binding domains in insects. *Insect Biochem Mol Biol.* 62:127–141.
- Thomas GWC, et al. 2020. Gene content evolution in the arthropods. *Genome Biol.* 21:15.
- Togawa T, Dunn WA, Emmons AC, Nagao J, Willis JH. 2008. Developmental expression patterns of cuticular protein genes with the R&R consensus from *Anopheles gambiae*. *Insect Biochem Mol Biol.* 38:508–519.
- Tomoyasu Y, Wheeler SR, Denell RE. 2005. *Ultrabithorax* is required for membranous wing identity in the beetle *Tribolium castaneum*. *Nature* 433:643–647.
- Vannini L, Willis JH. 2016. Immunolocalization of cuticular proteins in Johnston's Organ and the corneal lens of *Anopheles gambiae*. *Arthropod Struct Dev.* 45:519–535.
- Wang Y-W, Li Y-Z, Li G-Q, Wan P-J, Li C. 2019. Identification of cuticular protein genes in the Colorado potato beetle *Leptinotarsa decemlineata* (Coleoptera: Chrysomelidae). *J Econ Entomol.* 112:912–923.
- Wang T, Montell C. 2007. Phototransduction and retinal degeneration in *Drosophila*. *Pflugers Arch.* 454:821–847.
- Waterhouse RM, Tegenfeldt F, Li J, Zdobnov EM, Kriventseva EV. 2013. OrthoDB: a hierarchical catalog of animal, fungal and bacterial orthologs. *Nucleic Acids Res.* 41:D358–D365.
- Weber H. 1954. Grundriss der Insektenkunde. Stuttgart: Gustav Fischer Verlag.
- Willis JH. 1986. The paradigm of stage-specific gene sets in insect metamorphosis: time for revision. *Arch Insect Biochem Physiol.* 3:47–57.
- Willis JH. 2010. Structural cuticular proteins from arthropods: annotation, nomenclature, and sequence characteristics in the genomics era. *Insect Biochem Mol Biol.* 40:189–204.
- Willis JH. 2018. The evolution and metamorphosis of arthropod proteomics and genomics. *Annu Rev Entomol.* 63:1–13.
- Wistow G. 1993. Lens crystallins: gene recruitment and evolutionary dynamism. *Trends Biochem Sci.* 18:301–306.
- Wolsky A, Zamora R. 1960. The structure of the "pearl" eye of *Latheticus oryzae*. *Am Nat.* 94:309–312.
- Wool D. 1985. Blind flour beetles: variable eye phenotypes in the *microcephalic* (*mc*) mutant of *Tribolium castaneum* (Coleoptera, Tenebrionidae). *Isr J Entomol.* 19:201–210.
- Yang X, et al. 2009. Probing the *Drosophila* retinal determination gene network in *Tribolium* (II): the *Pax6* genes *eyeless* and *twin of eyeless*. *Dev Biol.* 333:215–227.
- Yang C-H, et al. 2017. Identification, expression pattern, and feature analysis of cuticular protein genes in the pine moth *Dendrolimus punctatus* (Lepidoptera: Lasiocampidae). *Insect Biochem Mol Biol.* 83:94–106.
- Yang X, Zarinkamar N, Bao R, Friedrich M. 2009. Probing the *Drosophila* retinal determination gene network in *Tribolium* (I): the early retinal genes *dachshund*, *eyes absent* and *sine oculis*. *Dev Biol.* 333:202–214.
- Zarinkamar N, et al. 2011. The Pax gene *eyegone* facilitates repression of eye development in *Tribolium*. *Evodevo* 2:8.
- Zhao X, et al. 2017. Identification and expression of cuticular protein genes based on *Locusta migratoria* transcriptome. *Sci Rep.* 7:45462.
- Zhou Y, et al. 2016. Distribution of cuticular proteins in different structures of adult *Anopheles gambiae*. *Insect Biochem Mol Biol.* 75:45–57.

Associate editor: George Zhang